Research Article | Vol. 25, No. 3 | 6 Feb 2017 | OPTICS EXPRESS 2038

Optics EXPRESS

Stokes space modulation format classification based on non-iterative clustering algorithm for coherent optical receivers

XIAOFENG MAI,[1,2] JIE LIU,[1,*] XIONG WU,[1] QUN ZHANG,[3] CHANGJIAN GUO,[4] YANFU YANG,[3] AND ZHAOHUI LI[1]

[1]*State Key Laboratory of Optoelectronic Materials and Technologies, School of Electronics and Information Technology, Sun Yat-Sen University, Guangzhou 510006, China*
[2]*School of Data and Computer Science, Sun Yat-Sen University, Guangzhou 510006, China*
[3]*Department of Electronic and Information Engineering, Shenzhen Graduate School, Harbin institute of Technology, Shenzhen 518055, China*
[4]*South China Academy of Advanced Optoelectronics, South China Normal University, Guangzhou 510006, China.*
[*]*liujie47@mail.sysu.edu.cn*

Abstract: A Stokes-space modulation format classification (MFC) technique is proposed for coherent optical receivers by using a non-iterative clustering algorithm. In the clustering algorithm, two simple parameters are calculated to help find the density peaks of the data points in Stokes space and no iteration is required. Correct MFC can be realized in numerical simulations among PM-QPSK, PM-8QAM, PM-16QAM, PM-32QAM and PM-64QAM signals within practical optical signal-to-noise ratio (OSNR) ranges. The performance of the proposed MFC algorithm is also compared with those of other schemes based on clustering algorithms. The simulation results show that good classification performance can be achieved using the proposed MFC scheme with moderate time complexity. Proof-of-concept experiments are finally implemented to demonstrate MFC among PM-QPSK/16QAM/64QAM signals, which confirm the feasibility of our proposed MFC scheme.

OCIS codes: (060.2330) Fiber optics communications; (060.1660) Coherent communications.

References and links

1. W. Wei, C. Wang, and J. Yu, "Cognitive optical networks: Key drivers, enabling techniques, and adaptive bandwidth services," IEEE Commun. Mag. **50**(1), 106–113 (2012).
2. K. Roberts and C. Laperle, "Flexible transceivers," in *European Conference and Exhibition on Optical Communication*, OSA Technical Digest (online) (Optical Society of America, 2012), paper We.3.A.3.
3. O. A. Dobre, A. Abdi, Y. Bar-Ness, and W. Su, "Survey of automatic modulation classification techniques: classical approaches and new trends," IET Commun. **1**(2), 137–156 (2007).
4. E. Ip, A. P. T. Lau, D. J. Barros, and J. M. Kahn, "Coherent detection in optical fiber systems," Opt. Express **16**(2), 753–791 (2008).
5. N. G. Gonzalez, D. Zibar, and I. T. Monroy, "Cognitive digital receiver for burst mode phase modulated radio over fiber links," in 36th *European Conference and Exhibition on Optical Communication,* Torino, 2010, pp.1–3.
6. F. N. Khan, Y. Zhou, A. P. Lau, and C. Lu, "Modulation format identification in heterogeneous fiber-optic networks using artificial neural networks," Opt. Express **20**(11), 12422–12431 (2012).
7. J. Liu, Z. Dong, K. P. Zhong, A. P. T. Lau, C. Lu, and Y. Lu, "Modulation format identification based on received signal power distributions for digital coherent receivers," in *Optical Fiber Communication Conference*, OSA Technical Digest (online) (Optical Society of America, 2014), paper Th4D.3.
8. R. Borkowski, D. Zibar, A. Caballero, V. Arlunno, and I. T. Monroy, "Optical modulation format recognition in stokes space for digital coherent receivers," in *Optical Fiber Communication Conference/National Fiber Optic Engineers Conference 2013*, OSA Technical Digest (online) (Optical Society of America, 2013), paper OTh3B.3.
9. R. Boada, R. Borkowski, and I. T. Monroy, "Clustering algorithms for Stokes space modulation format recognition," Opt. Express **23**(12), 15521–15531 (2015).
10. P. Isautier, J. Pan, and S. Ralph, "Robust autonomous software-defined coherent optical receiver," in *Optical Fiber Communication Conference*, OSA Technical Digest (online) (Optical Society of America, 2014), paper W1G.7.

#280585 http://dx.doi.org/10.1364/OE.25.002038
Journal © 2017 Received 21 Nov 2016; revised 5 Jan 2017; accepted 6 Jan 2017; published 25 Jan 2017

Optics EXPRESS

11. P. Isautier, J. Pan, R. DeSalvo, and S. E. Ralph, "Stokes space-based modulation format recognition for autonomous optical receivers," J. Lightwave Technol. **33**(24), 5157–5163 (2015).
12. T. Bo, J. Tang, and C. Chan, "Blind modulation format recognition for software-defined optical networks using image processing techniques," in *Optical Fiber Communication Conference*, OSA Technical Digest (online) (Optical Society of America, 2016), paper Th2A.31.
13. P. J. Winzer, A. H. Gnauck, C. R. Doerr, M. Magarini, and L. L. Buhl, "Spectrally efficient long-haul optical networking using 112-Gb/s polarization-multiplexed 16QAM," J. Lightwave Technol. **28**(4), 547–556 (2010).
14. C. Xie and G. Raybon, "Digital PLL based frequency offset compensation and carrier phase estimation for 16QAM coherent optical communication systems," in *European Conference and Exhibition on Optical Communication*, OSA Technical Digest (online) (Optical Society of America, 2012), paper Mo.1.A.2.
15. T. Pfau, S. Hoffmann, and R. No'e, "Hardware-efficient coherent digital receiver concept with feed forward carrier recovery for M-QAM constellations," J. Lightwave Technol. **27**(5), 989–999 (2009).
16. A. Rodriguez and A. Laio, "Clustering by fast search and find of density peaks," Science **344**(6191), 1492–1496 (2014).
17. I. Fatadin, S. J. Savory, and D. Ives, "Compensation of quadrature imbalance in an optical QPSK coherent receiver," IEEE Photonics Technol. Lett. **20**(20), 1733–1735 (2008).
18. T. Tanimura, S. Oda, T. Tanaka, T. Hoshida, Z. Tao, and J. C. Rasmussen, "A simple digital skew compensator for coherent receiver" in 2009 35th *European Conference on Optical Communication*, Vienna, 2009, pp. 1–2.
19. R. Kudo, T. Kobayashi, K. Ishihara, Y. Takatori, A. Sano, and Y. Miyamoto, "Coherent optical single carrier transmission using overlap frequency domain equalization for long-haul optical systems," J. Lightwave Technol. **27**(16), 3721–3728 (2009).
20. S. J. Savory, "Digital filters for coherent optical receivers," Opt. Express **16**(2), 804–817 (2008).
21. F. Gardner, "A BPSK/QPSK timing-error detector for sampled receivers," IEEE Trans. Commun. **34**(5), 423–429 (1986).
22. D. Godard, "Pass band timing recovery in an all-digital modem receiver," IEEE Trans. Commun. **26**(5), 517–523 (1978).
23. B. Szafraniec, B. Nebendahl, and T. Marshall, "Polarization demultiplexing in Stokes space," Opt. Express **18**(17), 17928–17939 (2010).
24. M. Chagnon, M. Osman, X. Xu, Q. Zhuge, and D. V. Plant, "Blind, fast and SOP independent polarization recovery for square dual polarization-MQAM formats and optical coherent receivers," Opt. Express **20**(25), 27847–27865 (2012).
25. C. M. Bishop, *Pattern Recognition and Machine Learning* (Information Science and Statistics, 2006).
26. A. P. Dempster, N. M. Laird, and D. B. Rubin, "Maximum likelihood from incomplete data via the EM algorithm," J. R. Stat. Soc. B **31**, 1–38 (1999).
27. J. L. Bentlet, "Multidimensional binary search trees used for associative searching," Commun. ACM **18**(9), 509–517 (1975).
28. G. Bosco, M. Visintin, P. Poggiolini, and F. Forghieri, "A novel update algorithm in stokes space for adaptive equalization in coherent receivers," in *Optical Fiber Communication Conference*, OSA Technical Digest (online) (Optical Society of America, 2014), paper Th3E.6.

1. Introduction

In order to further increase the spectral efficiency and assure the quality of service, the concept of cognitive optical networks (CON) [1] has been put forward in recent years. In CONs, cognitive abilities, such as adaptive modulation format and data rate to accommodate dynamic traffic requirements, are required at the transmitters of CONs [2]. Correspondingly, the knowledge of these kinds of adaptive parameters should be available at CON receivers. Particularly, it is essential for the receiver in CON to recognize or classify the modulation formats of the received signals autonomously, so that proper modulation-format-dependent digital signal processing (DSP) [4] can be employed subsequently to achieve the optimum performance.

Although modulation format classification (MFC) has been widely studied in wireless communication fields [3], it is worth revisiting the idea of MFC in fiber optical communications because of the unique channel impairments, such as fiber dispersion, fiber nonlinearities, crosstalk resulted from polarization rotation and large carrier phase noises, which will bring new challenges to optical MFC techniques. Several schemes were proposed for MFC of optical signals recently [5–12]. Among them, Stokes-space-based MFC for dual-polarization coherent optical receivers has attracted interests of many researchers, since it is inherently insensitive to carrier phase noise, frequency offset as well as polarization mixing [8–12]. As a result, MFC can be done at an early stage in the DSP module before the modulation format dependent algorithms (e.g. adaptive equalization for polarization

Optics EXPRESS

demultiplexing [13], frequency offset/carrier phase estimation [14,15], etc.). However, to the best of our knowledge, no results proved that MFC of 32QAM and 64QAM signals could be achieved in Stokes-space-based schemes in previous literatures [8–12]. Furthermore, iterated machine learning algorithms were required in some Stokes space MFC methods [8, 9], which increased the computation complexity.

Therefore, in this paper, a Stokes-space MFC technique based on non-iterative density-peak-search clustering algorithm is proposed for coherent optical receivers. The clustering algorithm utilized here is a modified form of the one proposed in [16]. With the introduction of a new parameter in the modified clustering algorithm, which is more suitable for Stokes space distributions of signals, performance of the proposed MFC can be improved. Successful MFC can be achieved among polarization multiplexed (PM) QPSK, 8QAM, 16QAM, 32QAM and 64QAM signals in numerical simulations. In addition, the performance of the proposed MFC algorithm is also compared with those of other schemes based on clustering algorithms. Simulation results show that good classification performance can be achieved using the proposed MFC scheme at the cost of moderate time complexity. Proof-of-concept experiments are carried out by exploiting MFC of PM-QPSK, PM-16QAM and PM-64QAM signals, which also confirm the feasibility of our proposed MFI technique in the dual-polarization long-distance fiber transmission systems.

2. Operating principle and simulation analysis

The placement of the proposed MFC technique in the DSP algorithm system designed for coherent optical receiver is shown in Fig. 1. In the DSP system, the conventional chromatic dispersion (CD) equalization and timing phase recovery algorithms are modulation-format independent [17–22], while the adaptive equalization for polarization demultiplexing, frequency offset compensation and carrier phase estimation algorithms are often depend on the modulation format [13–15]. As a result, the proposed MFC algorithm is placed after the modulation-format independent algorithms and before the modulation-format dependent algorithms, giving a prior knowledge of the modulation format to the subsequent algorithms.

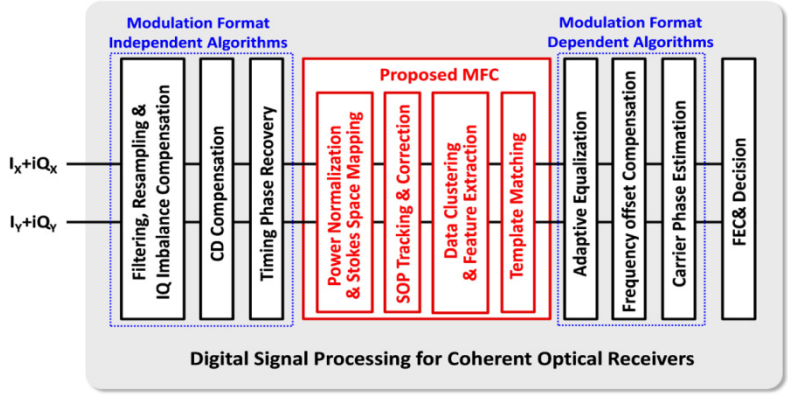

Fig. 1. Block diagram of DSP architecture with proposed MFC technique designed for coherent optical receivers

Four operating steps are included in our proposed scheme: Stokes space mapping, state of polarization (SOP) tracking and correction, identifying feature extraction based on density-peak clustering of the data points in Stokes space and the classifier algorithm based on template matching, as shown in Fig. 1. Here note that the random SOP needs to be tracked and rotated to its initial state in Stokes space to make sure the optimum performance of the proposed MFC. This process in Stokes space is modulation format independent and much easier than that in the Jones space [23,24]. Furthermore, the estimated polarization rotation

matrix in this process can then be used as an initial state of the subsequent adaptive equalization algorithm for polarization demultiplexing, which can greatly decrease the convergence time compared with that of the conventional constant modulus algorithm [24]. The MFC is still performed before polarization demultiplexing. Details of the MFC operating process as well as the simulation analysis will be described in the following parts of this section.

2.1 Stokes mapping and SOP correction

After CD equalization and timing phase recovery, the received polarization-multiplexed (PM) complex signals e_x and e_y (horizontal and vertical components of Jones vector [23]), both being power normalized, are mapped into Stokes space in the initial stage of MFC algorithm. The Stokes vector $\vec{S}$ of the k_{th} received symbol can be obtained using the following equation [23]:

$$\vec{S}(k)=\begin{pmatrix}s_0(k)\\ s_1(k)\\ s_2(k)\\ s_3(k)\end{pmatrix}=\begin{pmatrix}e_x(k)e_x^*(k)+e_y(k)e_y^*(k)\\ e_x(k)e_x^*(k)-e_y(k)e_y^*(k)\\ e_y(k)e_x^*(k)+e_x(k)e_y^*(k)\\ -je_y(k)e_x^*(k)+je_x(k)e_y^*(k)\end{pmatrix}=\begin{pmatrix}a_x^{\,2}(k)+a_y^{\,2}(k)\\ a_x^{\,2}(k)-a_y^{\,2}(k)\\ 2a_x(k)a_y(k)\cos\Delta\phi(k)\\ 2a_x(k)a_y(k)\sin\Delta\phi(k)\end{pmatrix} \quad (1)$$

Where $a_x(k)$ and $a_y(k)$ are the amplitudes of the complex symbols $e_x(k)$ and $e_y(k)$, respectively, while $\Delta\phi(k)$ is equivalent to the phase difference between $e_x(k)$ and $e_y(k)$.

The 3-D Stokes-space constellations can be obtained by using the last three components of the Stokes vector $(s_1,s_2,s_3)^T$. As was proved in [23], the Stokes-space constellations of the ideal PM symbols are confined within a lens-like object, which is independent on the modulation format. In addition, the symmetric plane of the lens-like object, called least square plane (LSP), can be obtained through least square fitting based on Singular Value Decomposition (SVD). The normal of the LSP, which contains polarization states of transmission, is utilized to realize SOP tracking and correction [23].

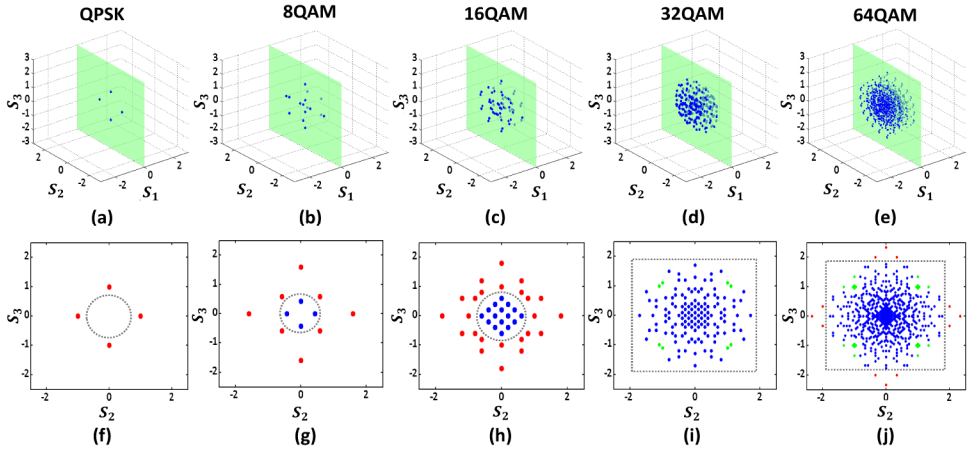

Fig. 2. Ideal constellations (a)-(e) in the 3-D Stokes space and (f)-(j) in the least square plane of the five modulation formats. The green plane in (a)-(e) means the least square plane.

The 3-D Stokes-space constellations of ideal PM-QPSK, PM-8QAM, PM-16QAM, PM-32QAM and PM-64QAM signals are illustrated in Figs. 2(a)-2(e), respectively. Comparatively, their distributions in the LSP are shown in Figs. 2(f)-2(j). Here note that the

Stokes-space constellations are mapped from symbols of the received PM signals (not include the transitions between symbols). And all the symbols are power normalized (mean power equals to one) before Stokes space mapping.

2.2 Feature extraction and non-iterative density peak clustering

As shown in Figs. 2(f)-2(j), signals with different modulation formats presents different characteristics of constellations in the LSP. For instance, there are points with both $|S_2|>1$ and $|S_3|>1$ in the LSP constellations of ideal PM-32QAM and PM-64QAM signals [green points in Figs. 2(i) and 2(j)], while these kinds of points do not exist for ideal PM-QPSK, PM-8QAM and PM-16QAM signals. Compared with other four kinds of signals under ideal conditions, there are LSP-constellation points with $|S_2|>2$ or $|S_3|>2$ for the 64QAM signals. These features can help classify the five modulation formats preliminarily. However, for the high-order multi-level modulation formats such as 32QAM and 64QAM, the density of the constellation points in the central region of LSP is so high that it is difficult to distinguish the constellation point in this area from others. This phenomenon indicates that it is necessary to select proper areas for data points clustering.

As a result, on the basis of the distribution features in the LSP, one parameter is defined to give preliminary classification of the five modulation formats, and two effective areas in the LSP are selected for data points clustering. The parameter R is defined as:

$$R=\frac{the\ number\ of\ in\ area\ \Omega}{the\ total\ number\ of\ points\ in\ the\ LSP} \tag{2}$$

Where Ω refers to the area with both $|S_2|>1$ and $|S_3|>1$ in the LSP. After choosing proper decision threshold, the five modulation formats can be divided into two groups {PM-QPSK, PM-8QAM, PM-16QAM} and {PM-32QAM, PM-64QAM} by utilizing the parameter *R*. About the clustering-area selection, we choose the points out of the circle whose radius is equal to 0.6 [as shown in Figs. 2(f)-2(h), the gray dot circle] for group {PM-QPSK, PM-8QAM, PM-16QAM}, and select the points out of the square whose length of side is equal to 3.6 [as shown in Figs. 2(i) and 2(j), the gray dot square] for group {PM-32QAM, PM-64QAM}.

In [16], the authors have proposed a non-iterative clustering algorithm to find density peaks of clusters with time-efficient and high-accurate performance, comparing with the conventional density-based clustering algorithm [25,26]. Two simple parameters of each data point are calculated to help find the cluster centers and no iteration is required. One of the parameters for the i_{th} data point, which is utilized to define the local density, is expressed as [16]:

$$\rho_i=\sum_{j}\chi(d_{ij}-d_c) \tag{3}$$

where d_{ij} denotes the distance between the j_{th} and the i_{th} data points and d_c is defined as the cutoff distance, which is with a fixed value in the algorithm. $\chi(x)$ is equal to 1 when x < 0 and equal to 0 otherwise. Therefore, ρ_i refers to the number of data points within a distance d_c. Evidently, larger ρ_i means higher local density of a data point. However, the value of ρ_i for data points in Stokes space depends on the distance from the origin. The outer data points in Stokes space are with much lower ρ_i for multi-level QAM signals. With low optical signal-to-noise ratios (OSNRs), outer Stokes-space constellations often have similar ρ_i with that of some noise points, which will degrade the performance of clustering algorithm (details will be discussed in section 2.4). As a result, to improve the performance of the clustering

algorithm utilized in our MFC module, a new parameter called local variance ψ is defined to take the place of ρ_i. Its value for the i_{th} point in the LSP can be calculated by:

$$\psi_i = \mathrm{var}(D_i) = \sqrt{\sum_{j=1}^{n}(d_j - \overline{D_i})^2}, d_j \in D_i \tag{4}$$

where D_i is a $1\times n$ matrix recording the distance between point i and its nearest n neighbors, d_j is the j_{th} element of D_i and $\overline{D_i}$ is the mean of D_i. It is noted that the n nearest neighbor searching algorithm called k-dimensional tree [27] is employed to get the matrix of D_i, which performs better than linear searching in terms of time complexity. Clearly, smaller value of ψ means higher density of the point. Therefore, the cluster centers (density peak of the cluster) have lowest ψ compared with other points at the same cluster.

The second parameter is the minimum distance δ, which can be given by:

$$\delta_i = \min_{j:\psi_j<\psi_i}(d_{ij}) \tag{5}$$

where δ_i means the minimum distance between point i and any other points with lower ψ. For the point with lowest local variance, we take $\delta_i = \max_j(d_{ij})$, which means that the distance between point i and the farthest point from it. After calculating both of the two parameters of each point, the point with relatively lower ψ and higher δ can be considered as the cluster centers. A 2-D picture called decision graph can be constructed if δ is regarded as the function of ψ. The position of cluster centers will be in the upper left part of the decision graph [see Fig. 3(d)].

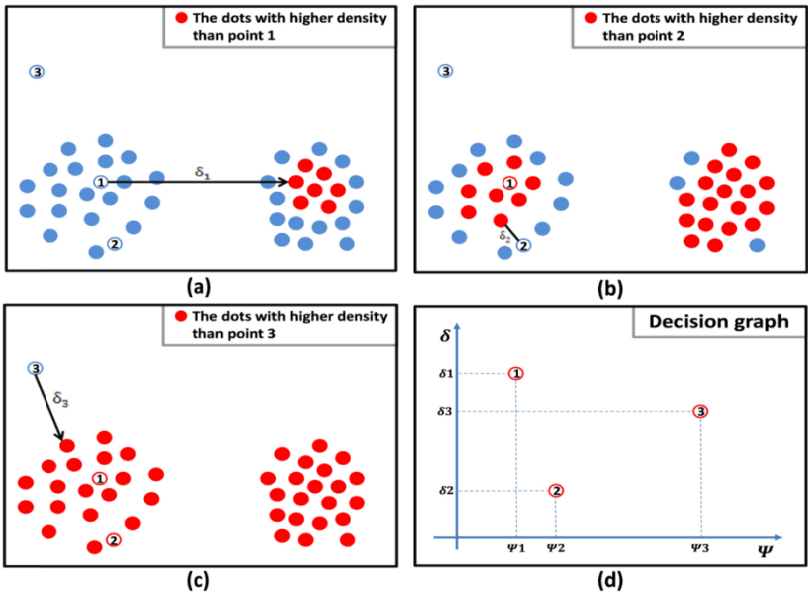

Fig. 3. (a)-(c): Schematic diagrams illustrating the minimum distances δ for three kinds of points; (d): decision graph

An example is given to illustrate how the algorithm works based on the two parameters and the decision graph. As shown in Figs. 3(a)-3(c), all the points can be divided into three

Optics EXPRESS

categories, which includes cluster centers (just like point 1), points with relatively lower local variance ψ (just like point 2) and outliers (just like point 3). These three types of points have different location in decision graph shown in Fig. 3(d). As the center of the left cluster depicted in Fig. 3(a), it is found that there is no other point with lower local variance ψ than point 1 in the same cluster. As a result, the points whose local variances are smaller than point 1 would be found in different clusters, for instance, the red points in the right cluster shown in Fig. 3(a). Hence the minimum distance δ of point 1, which stretches across two different clusters, is larger than those of other points in the same cluster. Therefore, cluster centers are with feature of low local variance ψ but high minimum distance δ. This is the reason why the cluster centers locate in the upper left part of the decision graph [see point 1 in Fig. 3(d)]. With respect to point 2, since it has relatively lower local variance than the cluster center (point 1), there must be points with smaller ψ in the same cluster. As a result its minimum distance δ will be less than that of point 1. As for point 3, namely outlier, there is no doubt that its local variance ψ is larger than other two kinds of points although it has relatively higher δ. Therefore, the location of point 3 is in the upper right part of the decision graph shown in Fig. 3(d). Consequently, cluster centers can be distinguished from other points using the location in decision graph in Fig. 3(d). By utilizing the proposed clustering algorithm, cluster centers of the constellation points in the LSP for the five modulation formats can be found at relatively high OSNRs, as the red points shown in Figs. 4(a)-4(e), which match the ones in Figs. 2(f)-2(j) quite well, respectively.

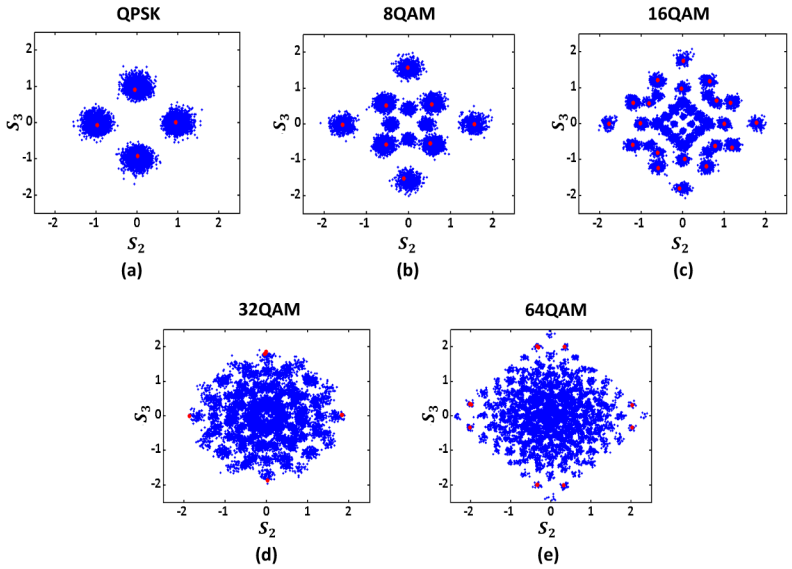

Fig. 4. Clustering results of the LSP constellations of the five different modulation formats at relatively high OSNRs. The red points mean the cluster centers.

2.3 Template matching

Stokes space constellations are sensitive to noise because of the noise probability density function distortion resulted from Stokes space mapping [28]. As a result, at low OSNRs, the number of clusters extracted using the proposed clustering algorithm is unsteady, even though proper areas in the LSP of Stokes space are selected for clustering. For instance, when it is at low OSNR, cluster number of the PM-8QAM signal in the area out of the circle with radius equal to 0.6 of the LSP [see Fig. 2(g)] will probably be five, which might be same with that of the PM-QPSK signal with large noise. This problem would also occur in the classification

between PM-8QAM and PM-16QAM signals. In this situation, successful classification cannot be realized between these modulation formats.

To solve such problem and improve the MFC performance, a simple method based on template matching is introduced, which compares the extracted cluster centers with the known standard templates of ideal PM-QPSK, PM-8QAM, PM-16QAM signals on the basis of the Euclidean distance summation expressed as:

$$distance(S,T)=\sum_{i=1}^{n}\left\|s_i-t_{nearest}\right\|^2, \qquad s_i \in S,\ t_{nearest} \in T_4, T_8 \text{ or } T_{16} \tag{6}$$

where S represents the set of extracted cluster centers with n elements. Each element refers to the position of one cluster center in the LSP. The sets of the points in templates of PM-QPSK, PM-8QAM and PM-16QAM signals are defined as T_4, T_8 and T_{16}, respectively. As one of the elements of the set T_4, T_8 or T_{16}, $t_{nearest}$ is the nearest point to s_i. Clearly, the best matching is determined according to the smallest value of the parameter *distance(S, T)*, and thus the modulation format is classified.

2.4 Simulation analysis

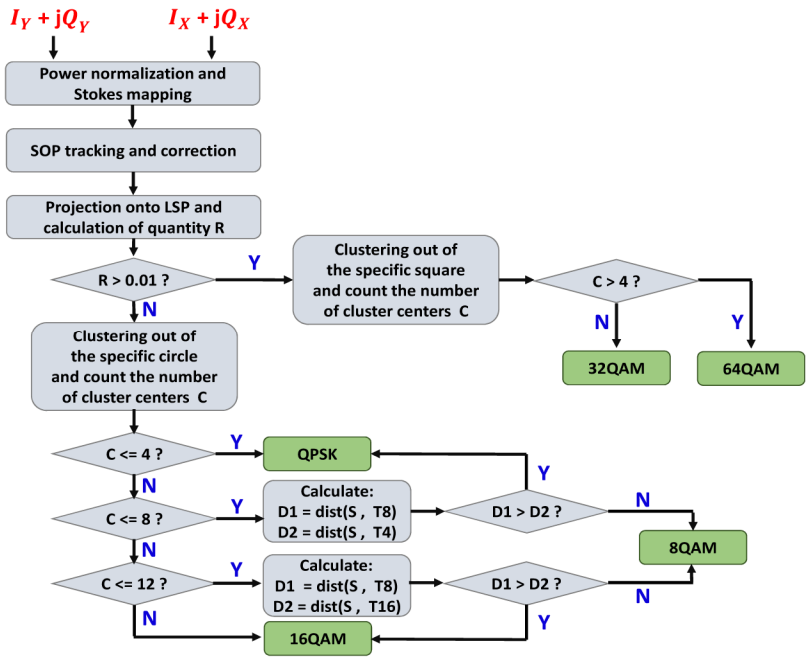

Fig. 5. Program flow chart for the proposed MFC technique.

Numerical simulations are performed to verify the performance of the proposed MFC technique. 28Gbaud PM-QPSK, PM-8QAM, PM-16QAM, PM-32QAM and PM-64QAM signals were generated and transmitted through a channel with additive Gaussian white noise. According to the program flow chart described in Fig. 5, 100 independent simulations were conducted for each OSNR value. Firstly, the performance of the proposed MFC technique using different numbers of test symbols at OSNRs approximating to their respective FEC thresholds was analyzed. The simulation results are shown in Fig. 6(a). It can be seen that 100% correct classification of the PM-64QAM signal can be realized with a minimum number of 8000 test symbols, while the same performance can be achieved for other four modulation formats with much less test symbols (their minimum number of test symbols are no more than 4000). As a result, in order to reduce the time complexity, 8000 symbols were

Optics EXPRESS

utilized for the test of PM-64QAM and PM-32QAM signals while 4000 symbols were employed for PM-QPSK, PM-8QAM and PM-16QAM signals in each run of our simulation. Here note that different number of test symbols can be employed for the two groups {PM-QPSK, PM-8QAM, PM-16QAM} and {PM-32QAM, PM-64QAM}, since the parameter R can be used to separate them in our scheme (see Fig. 5). Probabilities of correct format classification at different OSNRs are shown in Fig. 6(b). It can be seen that virtually 100% correct classification of the five modulation formats is achieved for OSNRs greater or equal to their respective forward error correction (FEC) thresholds. Here note that OSNR thresholds corresponding to FEC correcting bit error rate (BER) of 2.4e-2 in dual-polarization systems was utilized.

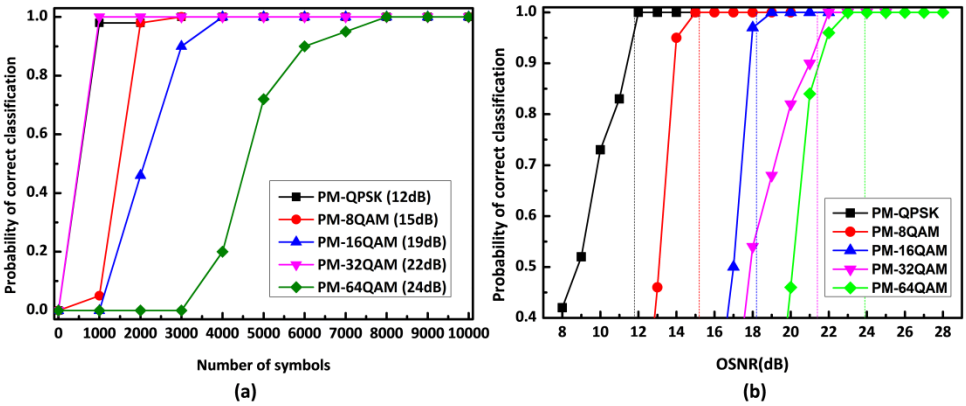

Fig. 6. Probability of correct classification at different (a) number of symbols; (b) OSNRs. The dotted lines (same color with the corresponding data curves) denote FEC thresholds of the corresponding modulation formats.

Taking the PM-16QAM signal as an example, the performance of the modified clustering algorithm used for MFC was also compared with that of original clustering algorithm proposed in [16]. As shown in insets of Fig. 7(a), cluster centers (red dots) extracted by the modified clustering algorithm at OSNR of 18dB are mainly located in the upper left part of the decision graph, which can be easily distinguished from other kinds of points if proper decision thresholds are chosen for local variance ψ and minimum distance δ. Comparatively, the distribution of cluster centers in the decision graph of the original clustering algorithm is more dispersed, increasing the difficulty of recognition of the cluster centers. As a result, when the probability of correct classification achieves around 100%, there are about 1-dB improvements of the MFC base on modified clustering algorithm, compared with that based on the original clustering algorithm.

In order to evaluate the proposed MFC scheme more comprehensively, performance comparisons between the proposed MFC algorithm and Stokes-space-based MFC schemes based on other clustering algorithms in [9] were implemented, by discriminating between the PM-QPSK, PM-8QAM and PM-16QAM signals. As shown in Fig. 7(b), the density-based spatial clustering of applications with noise (DBSCAN) and Maximum-likelihood (ML) based algorithms were selected for comparison due to their relatively lower complexity and higher OSNR performance, respectively, according to the analysis in [9]. The relative complexity of each algorithm illustrated in Fig. 7(b) was obtained by calculating average runtime and normalizing with regard to the longest time (ML based algorithm with QPSK). Here we note that 4000 symbols were utilized in each test of the proposed MFC algorithm based on non-iterative clustering, while 2000 test symbols (same number of symbols was used in [9]) were employed for the other two algorithms. Although more symbols were used than the other two algorithms, moderate runtime (around 7 times lower than the ML based method and 6 times higher than the DBSCAN based method) was needed for our proposed

Optics EXPRESS

MFC scheme. In addition, similar OSNR performance (minimum required OSNR to achieve reliability higher than 95%) could be achieved by using the proposed MFC algorithm, compared with that of the ML based scheme, which are better than that of the DBSCAN based method.

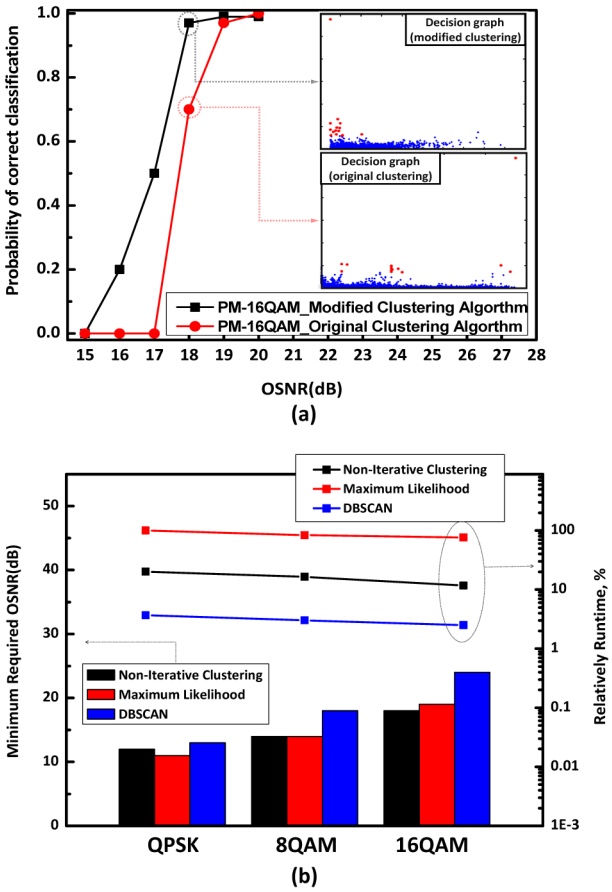

Fig. 7. (a) Probability of correct classification vs. OSNR for PM-16QAM signals. Insets: decision graphs for modified and original clustering algorithms; (b) time complexity and OSNR performance (minimum required OSNR to achieve reliability higher than 95%) comparisons between the proposed MFC algorithm and DBSCAN, ML based MFC algorithms.

3. Experimental verifications

A proof-of-concept experiment was conducted to prove the feasibility and evaluate the performance of the proposed MFC technique. Figure 8 shows the experimental setup, which consists of an optical baseband transmitter with single wavelength channel, a fiber re-circulating loop including an erbium-doped fiber amplifier (EDFA) and a 80-km standard single mode fiber (SSMF) span, and an integrated coherent optical receiver followed by a 50GSa/s real-time oscilloscope. At the transmitter, optical light from an external cavity laser (ECL) at 1550.92nm was modulated by 28GBaud QPSK, 28GBaud 16QAM and 20GBaud 64QAM signals generated from the arbitrary waveform generator (AWG) through an I/Q modulator to generate the optical signals. Then the optical signals are polarization multiplexed, which realized by through a polarization beam splitter (PBS), an optical delay line and a polarization beam combiner (PBC). After polarization multiplexing, the optical signals were amplified by an EDFA and launched into a fiber recirculating loop. At the

Optics EXPRESS

receiver, the optical signals were detected by the coherent optical receiver. Here note that the linewidth of the local oscillator (LO) is 100 kHz, same with that of the transmitting laser. Then the detected signals were sampled by the real-time oscilloscope and processed offline by algorithms including normalization, re-sampling, CD compensation and timing phase recovery to both of the two modulation formats and then sent to the MFC mechanism. In our experiments, over 40 discontinuous data were captured, to evaluate the MFC performance qualified by probabilities of correct format.

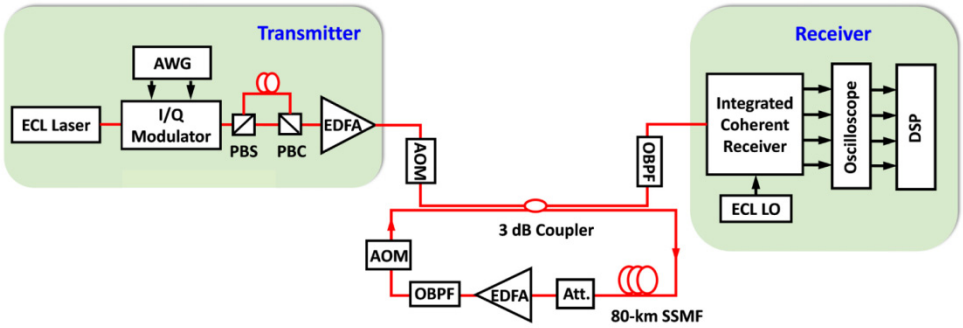

Fig. 8. Experimental Setup. AOM: acoustic-optic modulator; OBPF: optical band pass filter; Att.: tunable attenuator.

The probabilities of correct format classification at different number of test symbols in the case of back to back (BTB) are shown in Fig. 10(a). The minimum number of test symbols ensuring 100% correct classification for PM-64QAM signals increases to 10000, compared with the value of 8000 in the simulation results. This might be due to the distortions resulted from the electro-optical modulation and the noises of the electrical amplifier in our experiment. Therefore, 10000 symbols/polarization were utilized in each test of the PM-64QAM signals while this value in the test of PM-QPSK and PM-16QAM signals is set to 4000. The probabilities of correct format classification at different OSNRs in the case of back to back (BTB) are shown in Fig. 10(b). Similar performance can be achieved compared with simulation results shown in Fig. 6(b) for all of the three signals. Here it should be noted that the LSP constellations of the measured symbols have some rotations compared with those theoretical ones, as shown in Fig. 9(a)-9(c), which might be caused by the residual polarization rotation or relative delay between the two polarization channels in the experiment. These rotations will have an impact on template matching procedure of the proposed MFC technique, since in this procedure decisions are made based on deviation of the cluster centers from the theoretical LSP constellations. Therefore, it is necessary to correct these kinds of rotations before data clustering. We can search out the position of the corner following two simple steps: 1) 50 farthest points from the origin in the LSP are found out, after filtering out the noise points, which can be identified by utilizing the decision graph shown in Fig. 3(d); 2) then the 50 points are divided into four groups according to which corner they are located and the mean point of each group is determined, which approximately represents the position of each corner. Hereafter the smallest angle between the position vector of the mean point in each corner and the x axis can be calculated and all the data points in the LSP can be rotated by such an angle. The centers found by clustering after rotation correction are shown in Fig. 9(d)-9(f).

Optics EXPRESS

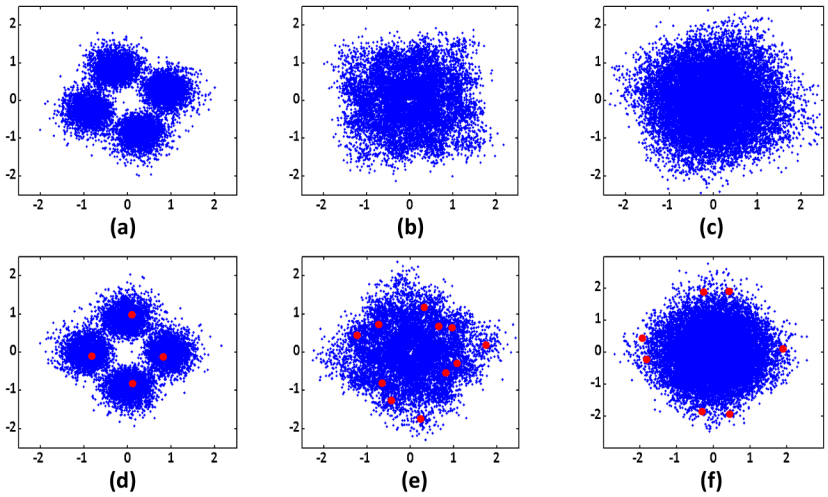

Fig. 9. LSP constellations in Stokes space before rotation correction: (a) PM-QPSK signals at OSNR of 12 dB; (b) PM-16QAM signals at OSNR of 18 dB; (c) PM-64QAM signals at OSNR of 24 dB, and after rotation correction: (d) PM-QPSK signals at OSNR of 12 dB; (e) PM-16QAM signals at OSNR of 18 dB; (f) PM-64QAM signals at OSNR of 24 dB (The red points mean the cluster centers).

Figure 10(c) shows probability of correct classification versus different signal power launched to optical fiber. With respect to the PM-QPSK signal after 1600-km transmission, 100% correct classification can be realized when the optical signal power launched to the fiber is up to 4 dBm. The same performance can be achieved for the PM-16QAM signal with 2-dBm optical power launched to the fiber after 1200-km transmission. Although there are some fluctuations for the probability of correct classification of the PM-64QAM signal after 320-km transmission when the test symbol number is equal to 10000, 95% correct classification can be assured within the range of the launched optical signal power to the fiber from −5 dBm to 4 dBm. The classification performance for PM-16QAM and PM-64QAM signals is improved when the test symbol number increases to 22000. As shown in Fig. 10(d), the fluctuation phenomenon of the measured curve of PM-64QAM signal disappears and the probability of correct classification of PM-16QAM signal can also be improved at low optical power launched to the fiber. There should be a tradeoff between the time complexity and the MFC performance.

Optics EXPRESS

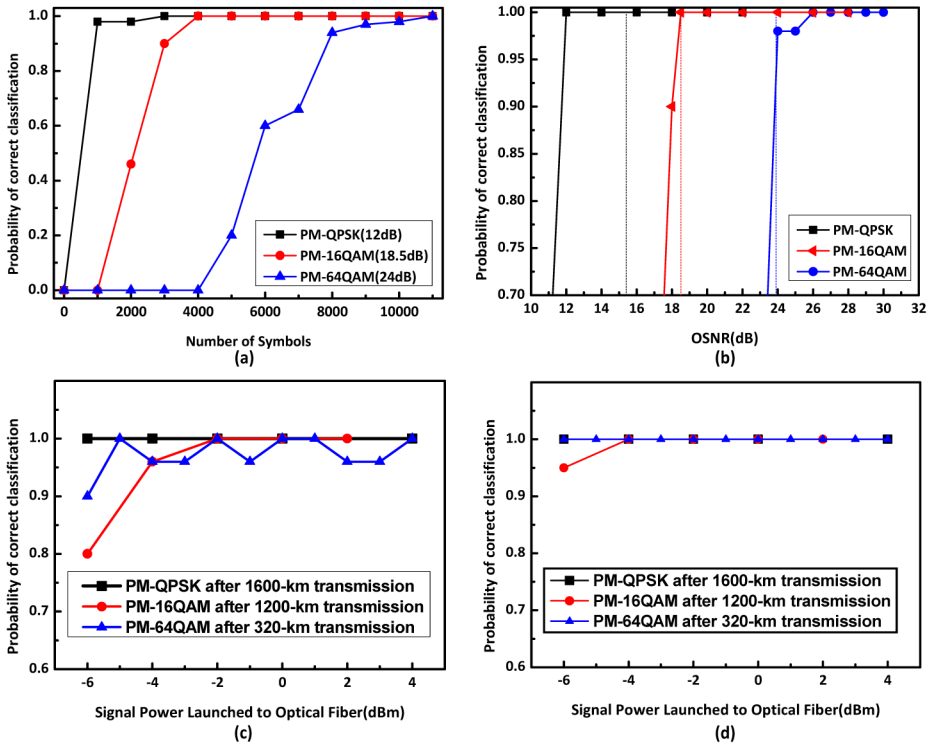

Fig. 10. Measured probability of correct classification vs. (a) number of test symbols; (b) OSNR in the case of back to back; signal power launched to optical fiber after fiber transmission (c) with 4000 test symbols for the PM-QPSK and PM-16QAM signals and 10000 test symbols for the PM-64QAM signal, and (d) with 22000 test symbols PM-QPSK, PM-16QAM and PM-64QAM signals.

4. Conclusions

We have proposed a Stokes space MFC technique based on the non-iterative density-peak-search clustering algorithm for digital coherent optical receivers. In the clustering algorithm, two simple parameters are calculated to help find the cluster centers of the data points in the LSP of Stokes space and no iteration is required. Successful MFC among PM-QPSK, PM-8QAM, PM-16QAM, PM-32QAM and PM-64QAM signals has been demonstrated in numerical simulations. Simulated performance comparisons between the proposed MFC algorithm and other MFC schemes based on clustering algorithm have also been implemented, showing that good classification performance can be achieved for the proposed MFC scheme with moderate time complexity. In the proof-of-concept experiment, PM-QPSK, PM-16QAM and PM-64QAM signals have been successfully classified both in the case of BTB and after long-distance fiber transmission.

Funding

This work was supported by Natural Science Foundation of China under grant No. 61505266 and Natural Science Foundation of Guangdong province, China under grant No. 2014A030310364 and grant No. 2016A030313289.